RSC Advances

ROYAL SOCIETY OF CHEMISTRY

www.rsc.org/advances

Cite this: DOI: 10.1039/c0xx00000x

www.rsc.org/xxxxxx

ARTICLE TYPE

Stereochemistry and Miscibility of Epoxy Resin-Poly (trimethylene terephthalate) Blends

Sarath Chandran,*[a, b] Antolaisic F[b], EichhornK J[c], Robert A Shanks[b] and S Thomas[a,b,c]

Received (in XXX, XXX) XthXXXXXXXXX 20XX, Accepted Xth XXXXXXXXX 20XX

DOI: 10.1039/b000000x

Abstract

Stereochemistry is proposed to contribute to miscibility of poly(trimethylene terephthalate) (PTT) and bisphenol-A diglycidyl ether (BADGE), since molecular conformation is a determinant of close packing ability and hence interactions. Polymer blends were prepared by the conventional melt mixing technique using a Haake mixer. The influence o f stereochemistry of the mixing polymers on miscibility is poorly investigated in literature. The amorphous fraction of PTT was found to be miscible with BADGE while the crystalline fraction is immiscible with BADGE. This is an interesting situation were one fraction of the polymer is miscible while another fraction is immiscible. The stereochemistry of the glycol residue of PTT is different in crystalline and amorphous fractions therefore miscibility of the amorphous fraction of PTT with BADGE can be due to the π-π and n-π interaction between the phenyl and carbonyl groups of PTT with the aromatic ring of BADGE. Fourier transform infra-red microscopy (FTIR Microscopy), Wide angle x-ray scattering (WAXS) and thermogravimetry shows that PTT and BADGE retain their identity in the blend eliminating the possibility any trans reaction between the blend components.

Introduction

The majority of the polymer pairs are found to be immiscible.[1] Development of sophisticated techniques to detect miscibility has resulted in an increase in the known number of miscible polymer blends.[1] Ultraki discussed the existence of around 1600 miscibility composition–temperature windows.[2] This shows that studies relating to the interaction between blend components is a topic of vital importance because the presence of interactions between the blend components has a dominating contribution to phase morphology and hence toward ultimate properties. Here we follow the miscibility of poly(trimethylene terephthalate) (PTT) in a bisphenol-A diglycidyl ether (BADGE) type of epoxy resin. The use of BADGE as a reactive compatibilizer for PTT-poly(butylene terephthalate) (PBT) has been reported earlier[3-5], but an in-depth investigation of the nature of interaction and the exact reason for the miscibility is missing.

Miscibility of many polyesters like poly(ethylene terephthalate) (PET)[6] and poly(butylene terephthalate) (PBT)[7] with BADGE has been reported. Reaction between the –OH and -COOH end groups of PET/PBT with oxirane ring of BADGE was used to explain the miscibility in these systems. The contribution of such a reaction towards miscibility is negligible due to two reasons: (1) The number of –OH and –COOH end groups are very low, (2) The experimental detection of the reaction is relatively difficult. A detailed investigation shows that the miscibility and behaviour of PTT towards BADGE is predominantly governed by the π-π and n-π interactions. PTT a higher homologue of PET and a lower homologue of PBT has a unique stereochemistry where the phenyl groups on the PTT chain can be considered as hard segments while the ether linked propane chain can be considered as soft segments. This gives rise to a helical structure that accounts for the exceptionally high resilience of PTT. Research shows that the *tggt* conformation of the soft segment corresponds to crystalline fraction while the *gttg* and all *trans* conformation corresponds to the amorphous fraction.[8-9] Thus the crystalline and amorphous fraction of PTT has different stereochemistry. The aim of the present research is to investigate the miscibility of PTT with BADGE. The possibility of reaction between PTT and BADGE is considered using differential scanning calorimetry (DSC), Fourier transform infrared (FT-IR) spectroscopy, Wide angle x-ray scattering (WAXS), and polarized optical microscopy (POM) while the thermal stability of the blends is investigated using thermogravimetry.

Experimental

Materials used

BADGE epoxy resin (Lapox L-12) with an epoxy equivalent between 5.25–5.40 eq·kg^{-1} and viscosity between 1.15–1.20 cm^2·s^{-1} was obtained from Atul Industries, Gujarat. Poly(trimethylene terephthalate) (PTT or Sorona 3G) with a density between 1.3–1.5 g·cm^{-3}, number average molecular weight ($\overline{M}_n$) of 22,500 g·mol^{-1} and polydispersity index (PDI) of 2.5 was kindly supplied by DuPont Industries, USA. Details of

the materials used are given in Table 1 and the chemical structure is shown in Figure 1.

All the materials were used as received without further purification. PTT-BADGE blends with varying amounts of PTT were prepared by a conventional melt mixing technique using a Thermo Fisher Rheomixer. Blends with and without curing agent were subjected to detailed analyses.

Blend preparation

Neat PTT pellets and PTT-BADGE blends with different amounts of BADGE (5, 10, 20 and 30 %·w/w) were mixed with a Thermo Fisher Rheomixer at a torque of 10 MPa, and temperature of 245 °C for 15 min. The blends prepared were compression moulded into sheets by pressing at 245 °C, and at 10 kPa, for 15 min. The blends were then subjected to detailed analysis and characterization.

Analysis

Differential scanning calorimetry

Differential scanning calorimetry (DSC) measurements were conducted using a Perkin Elmer Pyris 1 DSC. Blends prepared were subjected to the following studies:

(a) Glass transition temperature (T_g) measurement

T_g studies were performed on PTT, PTT-BADGE blends and BADGE using the PerkinElmer DSC. About 5 mg samples was accurately weighed using a Mettler microbalance, first heated to 260 °C at a heating rate of 10 K·min^{-1} and annealed for 3 min to remove any thermal history, followed by cooling to 20 °C at a rate of 10 K·min^{-1}. The sample was then again heated to 260 °C at 10 K·min^{-1}. Endothermic deviations from the baseline observed during the second heating cycle were noted.

(b) Equilibrium melting temperature (T_m°) studies

T_m° for PTT and PTT-BADGE blends were calculated by heating the samples to an annealing temperature (T_a) of 260 °C, followed by quenching to selected crystallization temperatures (T_c) and held at that T_c for 60 s. Each sample was then heated to 260 °C and the melting temperature (T_m) obtained during the second heating was used for analysis.

Wide angle x-ray scattering (WAXS) studies

WAXS analysis was carried out on PTT and PTT-BADGE blends using a Bruker d8 X-ray diffractometer equipped with a goniometer, between 2θ values of 10-35°.

Fourier transform infrared (FTIR) spectroscopy

FTIR spectroscopy studies on PTT and PTT-DGEBA blends was carried out using ATR (Golden Gate Unit), Bruker-FTIR spectrometer, as described by Aravind et al.[10]

Fourier transform infrared microscopy (FTIR Microscopy)

FTIR microscopy analysis was carried out on selected samples (neat PTT and 70 %·w/w blend) using a PerkinElmer FTIR microscope coupled to a Spectrum 1 FTIR spectrometer. Samples were studied using a germanium crystal, with 64 scans/pixel at a resolution of 16. The results obtained were analysed using PerkinElmer Spectrum Image software. Results obtained for neat PTT and the 70 %·w/w blend are presented here.

Polarized optical microscopy

Morphologies of neat PTT and PTT-BADGE blends (50-50) were imaged with a Nikon Labophot 2 microscope (Yokohama, Japan) equipped with a Linkam heating/cooling unit (Linkam TM 600/s) (Surrey, UK) with images collected using Leica Q Win software. Neat PTT and 50-50 blends were heated to 250 and 215 °C respectively and then cooled to 198 °C using liquid nitrogen atmosphere at a cooling rate of 50 K·min^{-1} and then held at that temperature for 1500 s.

Thermogravimetry (TGA)

TG analysis was carried out on PTT and PTT-BADGE blends using a PerkinElmer TGA7 instrument calibrated with Curie temperature metal standards. The samples were heated from room temperature to 800 °C at a heating rate of 10 K·min^{-1} in dry nitrogen atmosphere purge. Results obtained were analysed with Perkin Elmer Pyris software.

Results and Discussion

Glass transition temperature

Glass transition related to cooperative segmental motion involving about 50-100 backbone carbon atoms is an Ehrenfest type second order transition.[11] Glass transition exists between the glassy region and liquid super-cooled below its melting temperature. A single glass transition temperature for polymer blends indicated that the domain size (d_d) is between 2-15 nm.[11, 12] Thus a single T_g for polymer blends does not imply miscibility and in turn gives information about the state of dispersion.[11] T_g can be correlated with miscibility by using equations like Fox equation[13] Couchman equation,[14] Gordon-Taylor equation.[15] The DSC heating curves of PTT-BADGE blends are shown in Figure 2.

All the blends showed a single T_g and the experimentally observed T_g values were fitted with the Fox model (1).

$$\frac{1}{T_g} = \frac{W_A}{T_{gA}} + \frac{W_B}{T_{gB}} \quad (1)$$

Where W_A and W_B are the weight fractions of the neat polymers while T_{gA} and T_{gB} are the corresponding glass transition temperatures. The experimentally observed *Tg* values showed a large deviation from the Fox model as shown in Figure 3.

Such a deviation from the Fox model has been reported earlier for BADGE-PEO blends[16] therefore the contribution from crystalline fraction of PTT was reduced and the recalculated T_g values showed a better fit with the Fox equation. Contribution from the crystalline fraction was reduced using the equation (2)

$$W'_{(PTT)} = (W_{(PTT)} - X_c)/(1 - X_c) \quad (2)$$

Where $W'_{(PTT)}$ is the weight fraction of amorphous PTT in the blend, $W_{(PTT)}$ the actual weight fraction of PTT in the blend, and X_c is the crystallinity calculated from the DSC measurements. This result confirms that the amorphous fraction of PTT is miscible with BADGE. Similarly an increase in ΔT_g and ΔC_p values indicated an increased segmental mobility in the blends as the amount of BADGE increased. The experimentally observed T_g values shown in Figure 3 follow a negative deviation with a

pronounced "cusp" or discontinuity. The deviation of T_g from the linear behaviour is considered as a measure of the strength of interaction between the blend components.[17] A "cusp" or discontinuity in T_g was first observed by Kovacs et al.[17] and was explained using the free volume theory. Accordingly if the difference in T_g between the blend components is more than 50 degree, the free volume of the polymer with higher T_g will approach zero at certain critical temperature (T_c). The T_c and corresponding critical composition (ϕ_c) can be calculated using the equations (3) and (4) proposed by Kovacs.[17]

$$T_c = T_{g(PTT)} - \left(\frac{f_{(PTT)}}{\Delta\alpha_{(PTT)}}\right) \quad (3)$$

$$\phi_c = \frac{f_{(PTT)}}{\left[\Delta\alpha_{(BADGE)}\left(T_{g(PTT)} - T_{g(PTT)}\right) + f_{(PTT)}\left(1 - \Delta\alpha_{(BADGE)}/\Delta\alpha_{(PTT)}\right)\right]} \quad (4)$$

Where $f_{(PTT)}$ is the free volume of PTT at $T_{g(PTT)}$ and $\Delta\alpha_{(PTT)}$ is the difference between the volume expansion coefficients in the glassy and liquid states. It is significant to note that the observed cusp can be masked if the contribution of crystallinity is not taken into consideration which is found to match with the results shown in Figure 3.

Equilibrium melting temperature

Equilibrium melting temperature ($T_m°$) is one of the basic physical quantities of polymers and is defined as the melting temperature (T_m) of ideal crystals with infinite crystal size.[18] The DSC exotherm was used to calculate the equilibrium melting temperature ($T_m°$) using Hoffmann-Weeks equation[19](5).

$$T_m = \frac{T_c}{2\beta} + T_m^o\left[1 - \frac{1}{2\beta}\right] \quad (5)$$

Here T_m and T_c are the observed melting and crystallization temperatures respectively while β is the lamellar thickness. The T_m values obtained at different T_c are plotted against each other and from this the $T_m°$ is calculated by extrapolation to where $T_m = T_c$. Usually the addition of an amorphous component into a semi-crystalline polymer should result in a depression in $T_m°$ and this is usually observed.[19] Thus a plot of ($1/T_m°$-$1/T_m°$') against ϕ^2 should give a straight line with a –ve slope (where T_m^0' represents the equilibrium melting temperature of the blend), which can be used to calculate the interaction parameter between the blend components by the Nishi and Wang equation.[20,21] The experimentally observed T_m values for PTT-BADGE blends were plotted against T_c as shown in Figure 4 and the $T_m°$ was calculated. The calculated values of $T_m°$ are shown in Table 2. The $T_m°$ values calculated using the Hoffmann-Weeks method (ref. Figure 4) was plotted against volume fraction of BADGE (ϕ) as shown in Figure 5. This leads to the fact that a plot of ($1/T_m°$-$1/T_m°$') against ϕ^2 show a +ve deviation rather than the expected –ve deviation (for low amounts of BADGE). This means that the crystalline fraction of PTT is incompatible with BADGE. On increasing the amount of BADGE above 20 %·w/w, BADGE enters into the PTT spherulites resulting in change in morphology of the PTT as observed in the decrease in lamellar thickness shown in Table 3 using WAXS studies. This can be due to the entropy contribution associated with the low molecular weight of BADGE. This conclusion of change in morphology was confirmed by the POM images (refer Figure 13).

Thus in PTT-BADGE we have two situations; an amorphous fraction which is miscible with BADGE and a crystalline fraction that is immiscible with BADGE. This situation can be envisaged on the basis of the fact that the crystallization of PTT results in an expulsion of BADGE from the intra-spherulitic region to the inter-spherulitic region. Optical micrograph for 50 %·w/w blend after 3600 sec of crystallization at 186 °C shown in Figure 6 confirms this argument. The inter-spherulitic region where amorphous fractions of PTT and BADGE localize is shown in black circles. The reason behind the selection of 50 %·w/w blend was that it showed more visible regions when compared to others with lower amounts of BADGE. Wide angle X-ray scattering studies (WAXS) on PTT-BADGE blends shows that PTT retains its unit cell dimensions, which rules out the possibility of any trans reaction between PTT and BADGE. Figure 7 shows the diffraction pattern observed for PTT with varying amounts of BADGE. WAXS plots show that the intensity of the diffraction peaks (010- 012) increase as the amount of BADGE increases, indicating slight changes in the unit cell dimensions that can be neglected. The peak width at half maximum height ($W_{1/2}$) gives indirect information about the lamellar thickness. The diffraction peak at (010) was taken for this calculation. $W_{1/2}$ for neat PTT and for PTT–BADGE blends shows an increase while the lamellar thickness decreases. The lamellar thickness was calculated using the Scherer equation (7).

$$t = \frac{0.9\lambda}{B\cos\theta} \quad (7)$$

Here t is the lamellar thickness, λ= 0.154 nm is the wavelength of the X-ray, B is the full width at half maximum (FWHM), while θ is the scattering angle corresponding to the peak under selection. The lamellar thickness values shown in Table 3 follow a decrease as the amount of BADGE in the blends increases, which can be due to two reasons (1) higher loadings of BADGE the morphology of PTT spherulites changes to a sheaf-like or dendrimeric structure, (2) increasing amounts of BADGE reduces the crystallization of PTT which in turn increases the amount of amorphous fraction of PTT. The FTIR spectra of PTT has been studied in detail by different groups[9,22] and it is concluded that the peaks at 933, 947, 1037, 1358 and 1465 cm^{-1} correspond to the crystalline fraction of PTT while the peaks at 811, 976, 1173, 1328, 1385, 1452, and 1577 cm^{-1} correspond to the amorphous fraction. It is assumed that in the crystalline fractions the stereochemistry of the glycol residue (soft segment) is predominantly *tggt*, whereas in the amorphous fraction the stereochemistry of the soft segment is *gttg* and all *trans*. This result was further confirmed by photoluminescence studies at different temperatures.[23] The above studies show that the *tggt* conformation results in the arrangement of the phenyl rings at a distance of 0.36 nm and thereby the π-π interactions between the phenyl rings assist crystallization. The FTIR spectra of neat PTT and PTT-BADGE blends are shown in Figure 8. The results obtained were used to calculate the blend mixing ratio and the amount of gauche conformation in PTT and PTT-BADGE

blends. In the calculation of blend composition using FTIR spectroscopy, peaks at 826 cm^{-1} (819 cm^{-1} in the blend) C-H out-of plane aromatic ring (p-phenyl) and 730 cm^{-1} (rocking due to aromatic ring) were used as the internal reference[10,24] and can be considered as constant internal standards for the calculation of the blend mixing ratio. Calculated blend mixing ratio is presented in Figure 9, and this shows a linear relation (within the error range) confirming the blend composition. The amount of gauche confirmation in amorphous and crystalline fraction of PTT can be obtained from the ratio A_{1358}/A_{1504}. A plot of A_{1358}/A_{1504} against the amount of BADGE shows a decrease as the amount of BADGE increases as shown in Figure 10. This confirms the presence of weak interaction between PTT and BADGE. The possibility of reaction between the hydroxyl (-OH) and carboxylic acid (-COOH) end groups of PTT with the epoxy group of BADGE was studied in detail and is incorporated here to answer the reviewers comment. For this the peaks at 826cm^{-1}, 913cm^{-1} and 1507cm^{-1} were considered. An almost linear fit observed within the error range for A_{913}/A_{1507} and A_{913}/A_{826} plotted against the amount of BADGE (refer Figure 11) confirms that the contribution of such a reaction towards miscibility is negligible. Thus the contribution of chemical reaction between the end groups of PTT and BADGE towards miscibility can be neglected. The FTIR microscopy images for neat PTT shows the presence of only one spectrum as expected. A chemimap image along with the spectra at different regions of the specimen is shown in Figure 12. The FTIR microscopy image of the 70 %·w/w blend given in Figure 13 shows the presence of two regions, (1) PTT that is the matrix and (2) dispersed BADGE droplets. This confirms our statement that the crystallization of PTT results in an expulsion of BADGE from the intra-spherulitic region to the inter-spherulite region. POM images of neat PTT and 50-50 blends are shown in Figure 14. Neat PTT showed a banded spherulite structure with well-defined maltese crosses, whereas in the case of 50-50 blends the bands disappeared. The 50-50 blends showed a well-defined maltese crosses and dendrimeric spherulites. This can be due to the fact that the excess BADGE causes a swelling of the PTT lamellae. TGA analysis on PTT-BADGE blends shows that the addition of BADGE has little effect on the degradation temperature of PTT as shown in Figure 15. The interesting conclusion here is that as the amount of BADGE increases slowly the degradation of BADGE starts to appear as shown in the Figure 15(b). Thus until 90 %·w/w there is a single stage degradation after which is observed a two stage degradation with the first degradation occurring at a temperature close to that of BADGE. The above discussion leads to the conclusion that the amorphous fraction of PTT is miscible with BADGE while the crystalline fraction is immiscible with BADGE. This can be explained using the schematic given in Figure 16. In the homogenous melt there is a uniform distribution of BADE as shown in Figure 16 (a). On cooling the *tggt* confirmation of the crystalline fraction result in effective packing that results in expulsion of BADGE from the intra-spherulitic region to the inter-spherulitic space, resulting in a decrease in interaction between PTT and BADGE as shown in Figure 16(c). The Figure 16 represents the situations that can be expected during the mixing of PTT with BADGE. In the molten state the BADGE monomers are expected to be distributed uniformly throughout the amorphous PTT matrix this is shown in Figure 16 (a) with the blue droplets representing BADGE monomers. With crystallization the packing of PTT lamellae causes an expulsion of BADGE monomers and amorphous fractions of PTT which is miscible with BADGE is shown in blue colour in Figure 16 (b) and 16 (c). The expected reason for the miscibility of the amorphous fraction of PTT with BADGE monomers can be envisaged as shown in Figure 16 (d). The more open structure of amorphous PTT (the *gttg* and all *trans* conformations) allows extensive interaction with BADGE resulting in miscibility while the opposite can be expected for the crystalline fractions of PTT as shown in figure 16 (e)

Conclusions

The influence of stereochemistry of the thermoplastic polyester PTT on its miscibility with BADGE has been investigated. T_g studies show that the blends behaviour is described by the Fox equation when crystallinity is excluded from the blend weight fractions. This indicates that the amorphous fractions of PTT are miscible with BADGE. $T_m°$ shows a slight increase that points toward incompatibility that is, the crystalline fractions are immiscible with BADGE. This apparent change in miscibility can be explained by the fact that the *tggt* conformation of the soft segments of PTT result in effective packing that reduces the possibility of interaction between the PTT and BADGE. Whereas the *gttg* and all *trans* conformations of the amorphous fractions of PTT result in a more open structure that induces greater the π-π and n-π interaction between PTT and BADGE. WAXS studies show that the lamellar thickness gradually decreases as the amount of BADGE in the blends increases. Thus at higher loadings of BADGE a change in morphology of PTT crystals is expected and this is in exact correlation with the POM results.TGA analysis shows the presence of multiple decomposition peaks, the lower decomposition peak corresponded to that of BADGE while the decomposition at higher temperature corresponded to that of PTT. The intensity of the lower decomposition peak increases as the amount of BADGE in the blends increases. The FTIR microscopy results show the presence of two different regions that indicate two results; (1) no possibility of any reaction between the PTT and BADGE at higher compositions, (2) crystallization of PTT results in an expulsion of BADGE from the intra-spherulite region to the inter-spherulite region. Thus the stereochemistry of the polymers plays a major role in deciding the miscibility. The results obtained are extremely important in the fabrication of novel materials with smart applications and further studies into this relationship are in progress.

Notes

[a]*Centre for Nanoscience and Nanotechnology, & School of Chemical Sciences, Mahatma Gandhi University, Kottayam, Kerala, India E-mail: sarathchandranc1@gmail.com , sabuchathukulam@yahoo.co.uk*
[b]*School of Applied Sciences, RMIT University, Melbourne, VIC 3000, Australia; E-mail: robert.shanks@rmit.edu.au*
[c]*Leibniz Institut für Polymerforschung Dresden e.V., TeilinstitutMakromolekulare Chemie, Abt. Analytik,Hohe Str. 6, 01069 Dresden.*

References

1 L. M. Robeson in *Polymer blends: a comprehensive review*, ed. L. M. Robeson, Hanser Verlag, Cincinnati, 2007, **2**, pp. 11-54.

2 G. Groueninckx, M. Vanneste, V. Evaraert in Polymer blends handbook , ed. L. A. Utracki, Kluwer Academic Pub, The Netherlands, 2nd edn., 2002, **2**, ch. 3, pp. 203-289.

3 M. L. Xue, Y. L. Yu, H. H. Chuah, G. X. Qiu, *Journal of Macromolecular Science, Part B: Physics,* 2007**,46**, 387-401.

4 M. L. Xue, Y. L. Yu, J. Sheng, H. H. Chuah, C. H. Geng, *Journal of Macromolecular Science, Part B: Physics,* 2005**,44**, 317-329.

5 M. L. Xue, Y. L. Yu, H. H. Chuah, *Journal of Macromolecular Science, Part B: Physics,* 2007**,46**, 603-615.

6 P. Huang, Z. Zhong, S. Zheng, W. Zhu, Q. Guo, *Journal of applied polymer science,* 1999**,73**, 639-647.

7 H. Zhang, M. Ren, Q. Chen, S. Sun, H. Zhang, Z. Mo, *Journal of Polymer Science Part B: Polymer Physics,* 2006**,44**, 1320-1330.

8 H. H. Chuah, *Macromolecules,* 2001**,34**, 6985-6993.

9 M. Yamen, S. Ozkaya, N. Vasanthan, *Journal of Polymer Science Part B: Polymer Physics,* 2008**,46**, 1497-1504.

10 I. Aravind, K. J. Eichhorn, H. Komber, D. Jehnichen, N. Zafeiropoulos, K. H. Ahn, Y. Grohens, M. Stamm, S. Thomas, *The Journal of Physical Chemistry B,* 2009**,113**, 1569-1578.

11 L. Utracki, *Advances in Polymer Technology,* 1985**,5**, 33-39.

12 K. Frisch, D. Klempner, H. Frisch, *Polymer Engineering & Science,* 1982**,22**, 1143-1152.

13 T. Fox, *Bull Am Phys Soc* ,1956**,1**, 123-123.

14 P. Couchman, *Macromolecules,* 1980**,13**, 1272-1276.

15 M. Gordon, J. S. Taylor, *Journal of Applied Chemistry,* 1952**,2**, 493-500.

16 Q. Guo, C. Harrats, G. Groeninckx, M. Koch, *Polymer* ,2001**,42**, 4127-4140.

17 M. Aubin, R. E. Prud'Homme, *Macromolecules,* 1988**,21**, 2945-2949.

18 K. Yamada, M. Hikosaka, A. Toda, S. Yamazaki, K. Tagashira, *Macromolecules,* 2003**,36**, 4790-4801.

19 H. Marand, J. Xu, S. Srinivas, *Macromolecules,* 1998**,*31***, 8219-8229.

20 T. Nishi, T. Wang, *Macromolecules,* 1975**,8,** 909-915

21 T. Nishi, T. Wang, T. Kwei, *Macromolecules* ,1975**,*8***, 227-234.

22 H. H. Chuah, *Macromolecules,* 2001**,34,** 6985-6993.

23 W-a Luo, Y. Chen, X. Chen, Z. Liao, K. Mai, M. Zhang, *Macromolecules,* 2008**,41**, 3912-3918.

24 A. Synytska, S. Michel, D. Pleul, C. Bellmann, R. Schinner, K. J. Eichhorn, K. Grundke, A. Neumann, M. Stamm, *The Journal of Adhesion,* 2004**,80**, 667-683

Table 1: Characteristics of PTT and BADGE used for this study

	PTT	BADGE
$\overline{M}_w$ [(a)] (g·mol^{-1})	58,400	-
$\overline{M}_n$ [(a)] (g·mol^{-1})	22,500	-
Viscosity[(b)] (cm^2·s^{-1})	-	1.15-1.20
Epoxy content[(b)] (equ·kg^{-1})	-	5.2- 5.4
Tg[(c)] (°C)	52.5	-16
T_m[(d)] (°C)	227	-
ΔH_{ref}[(e)](J·g^{-1})	146	-
Supplier	DuPont Industries, USA.	Atul Industries, Gujarat, India.

a. Molar mass as estimated in this work by GPC (Perkin-Elmer), polystyrene with low polydispersity was used as standard.
b. Information provided by the supplier.
c. Glass transition temperature as determined in this work by mT-DSC.
d. Apparent melting temperature for the neat polymer during a first heating scan by DSC.
e. The melting enthalpy of 100 % crystalline PTT crystals

Table 2: T_m° along with the slope (α) and correlation coefficient (r) for PTT-BADGE blends

%·w/w of BADGE	T_m° / °C	α	r
0	231.8	0.490	0.853
5	232.1	0.476	0.990
10	232.4	0.573	0.995
20	232.6	0.660	0.998
30	218.6	0.490	0.915

Table 3: Variation of $W_{1/2}$ and lamellar thickness as a function of the amount of BADGE

Composition (%·w/w)	Peak width at half maximum ($W_{1/2}$) (°)	Lamellar thickness t (nm)
0	0.2814	2846.9
5	0.2926	2737.9
10	0.3729	2148.3
20	0.3202	2501.9
30	0.3206	2498.8
50	0.4396	1822.1

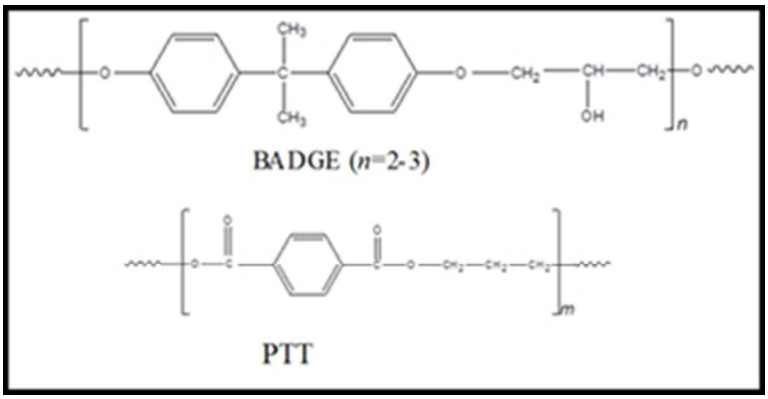

Chemical structure of PTT and BADGE (n≠ m)
189x94mm (51 x 52 DPI)

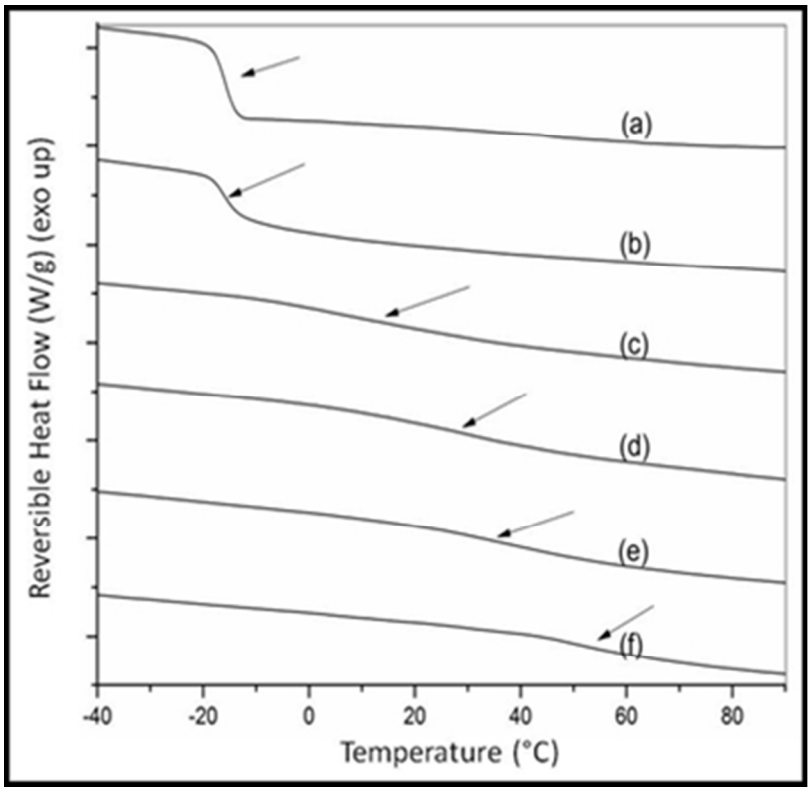

MTDSC curves for PTT-BADGE blends where (a) neat BADGE, (b) 50 %•w/w of BADGE, (c) 30 %•w/w of BADGE, (d) 20 %•w/w of BADGE, (e) 10 % w/w of BADGE, (f) neat PTT
161x157mm (63 x 63 DPI)

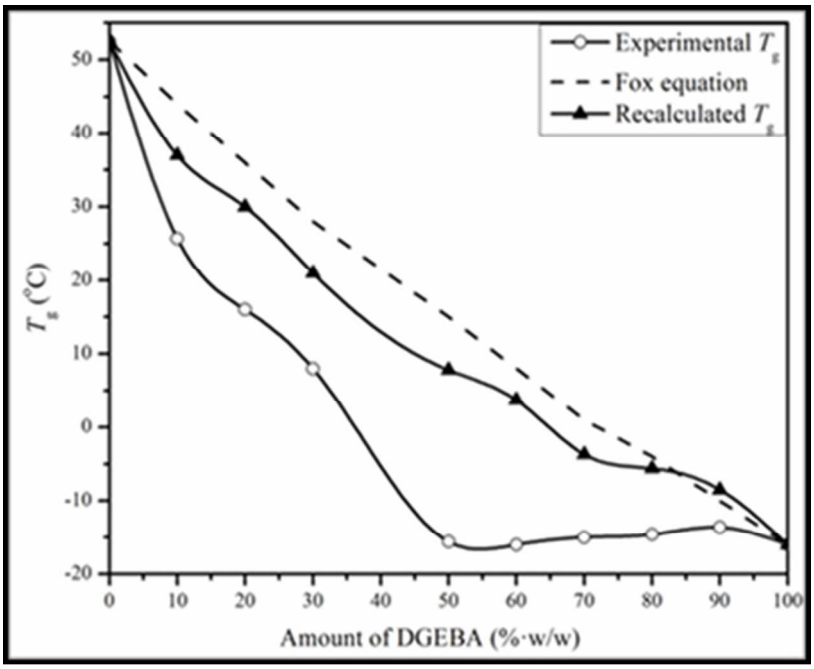

Tg values for PTT-BADGE blends as a function of the BADGE composition
146x119mm (70 x 70 DPI)

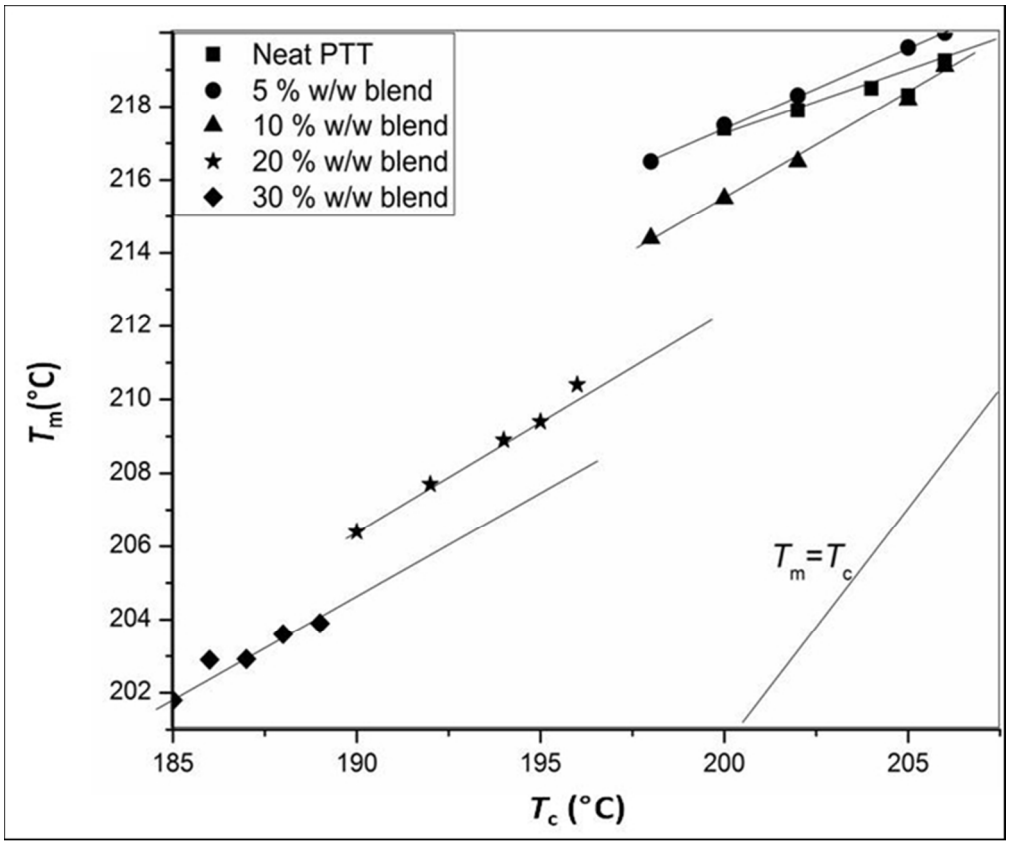

Tm against Tc curves for PTT–BADGE blends
133x104mm (140 x 150 DPI)

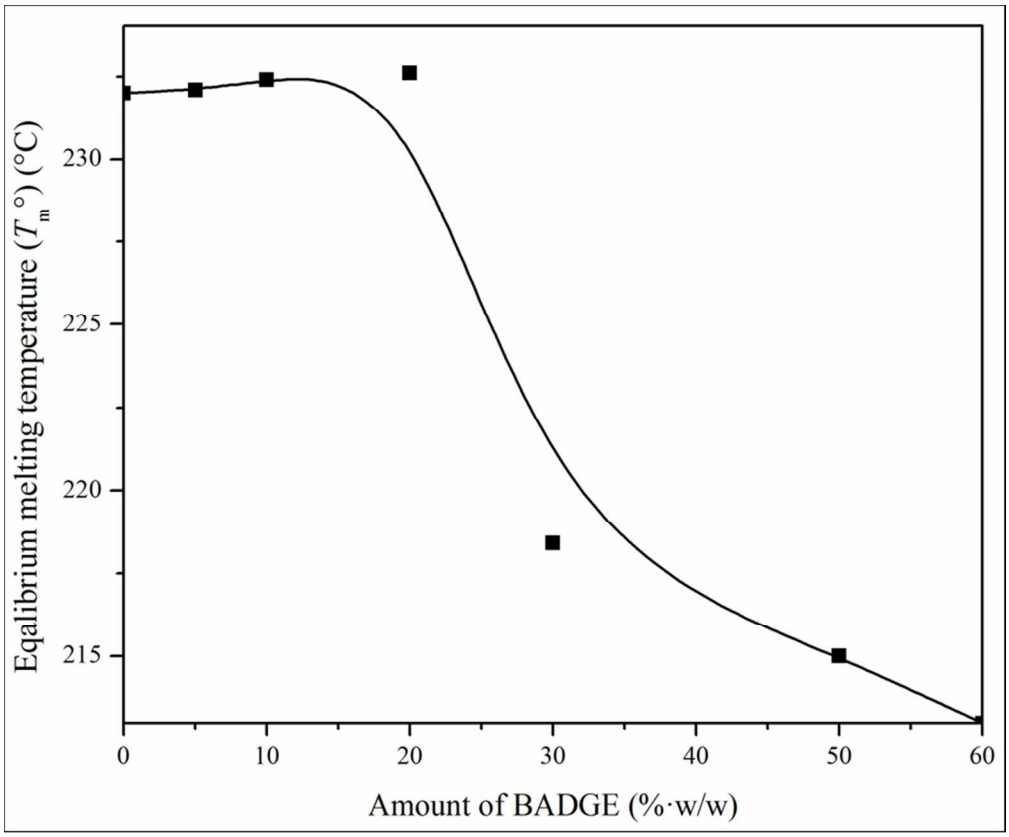

Plot of Tm° against composition of BAGDE for PTT-BADGE blends
159x131mm (150 x 150 DPI)

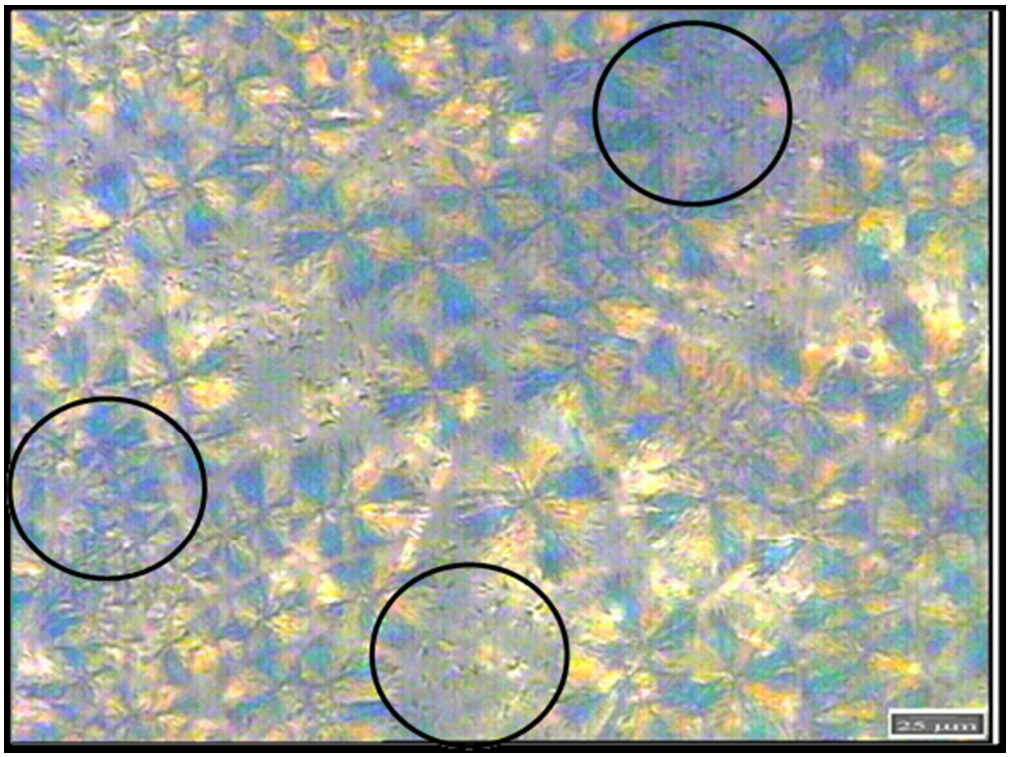

POM image for 50 %•w/w blend after 3600 sec at a crystallization temperature of 186 °C
140x117mm (104 x 93 DPI)

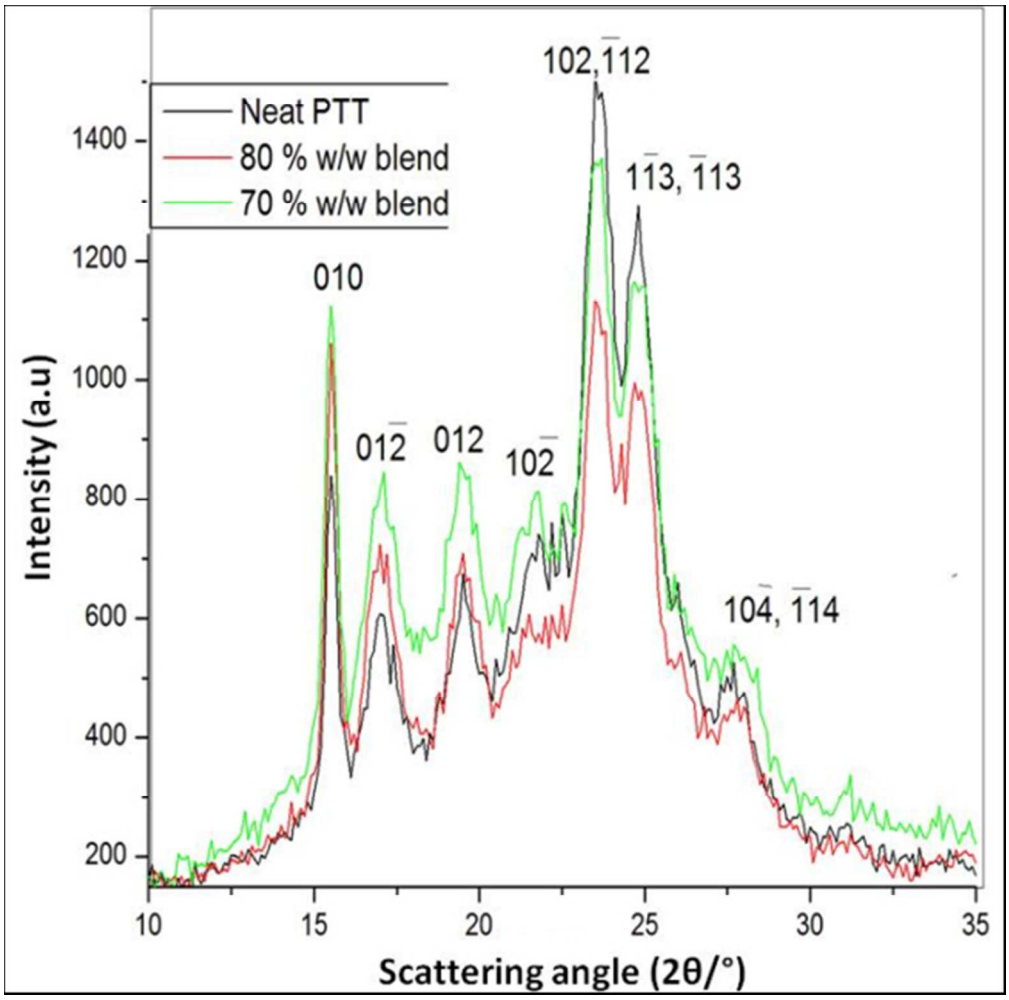

WAXS profile for PTT-BADGE blends
171x135mm (96 x 120 DPI)

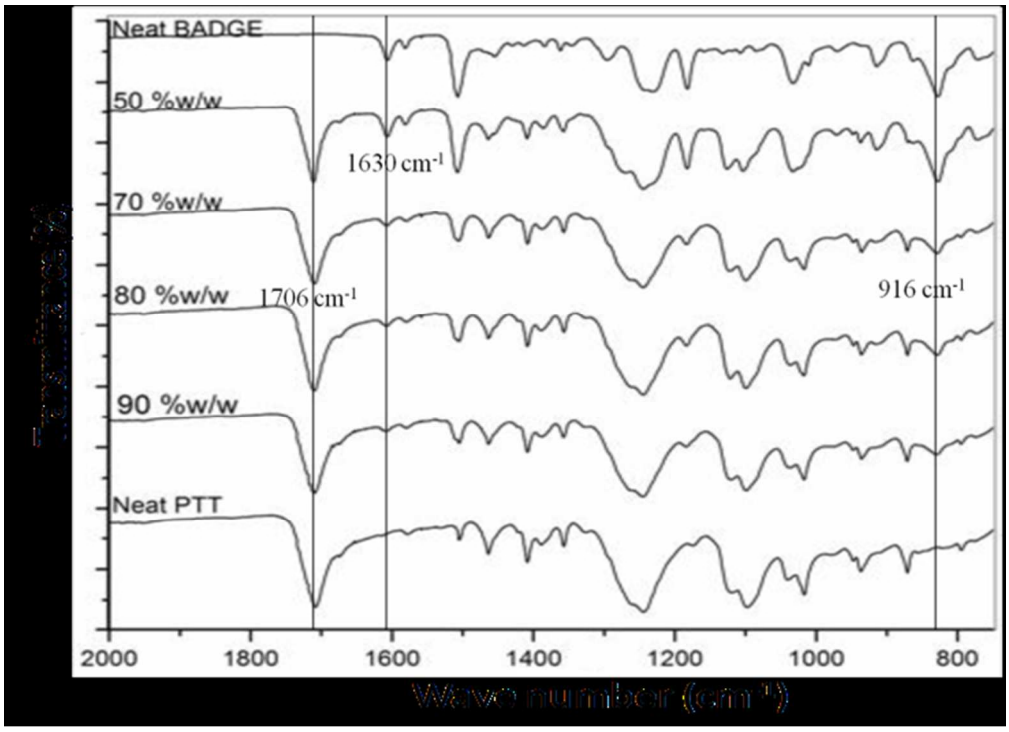

FTIR spectra of PTT and PTT-BADGE blends
174x131mm (107 x 102 DPI)

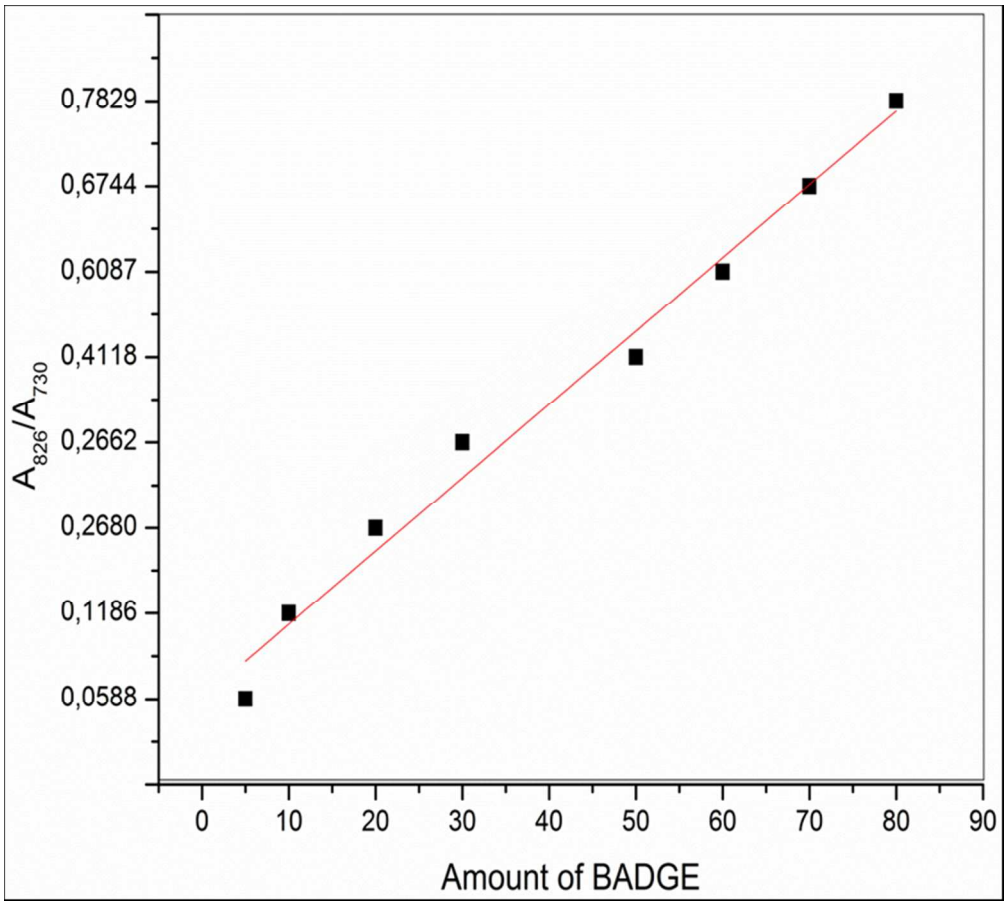

Ratio of the absorbance peak (A826/A730) against the amount of BADGE for PTT-BADGE blends
140x125mm (150 x 150 DPI)

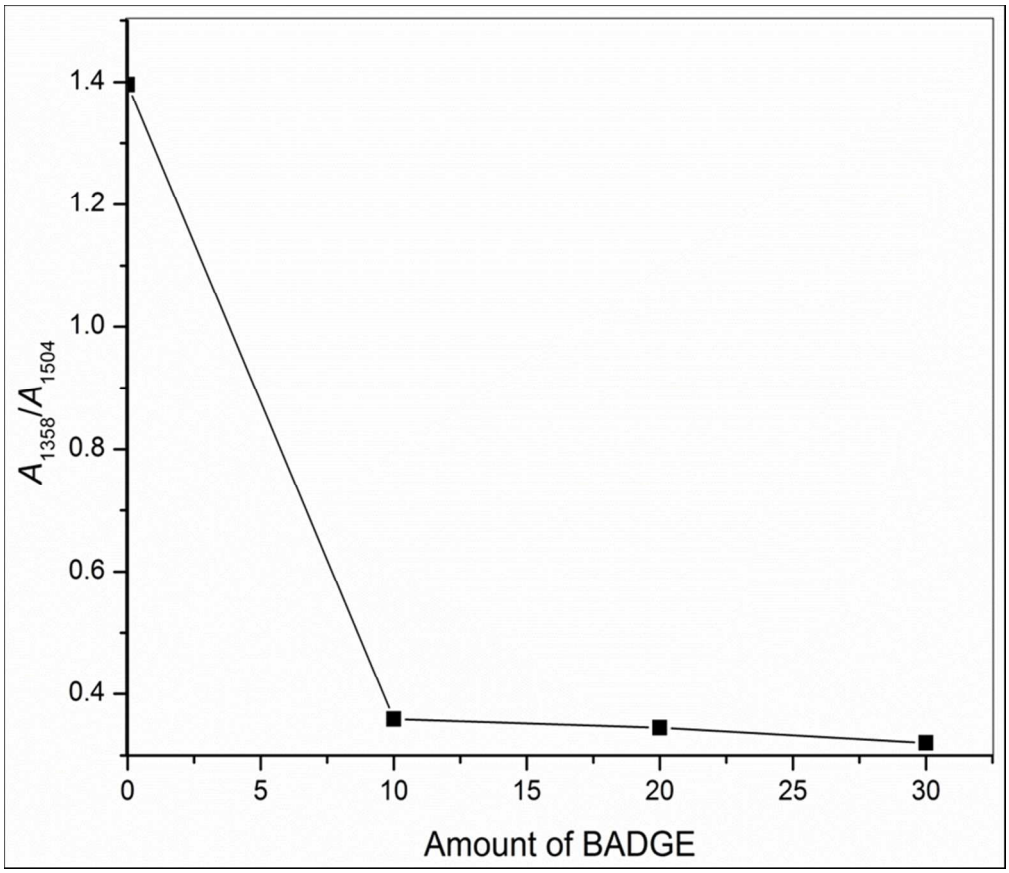

Ratio of the absorbance at 1358 to 1504 cm-1 for neat PTT and PTT–BADGE blends
154x133mm (150 x 150 DPI)

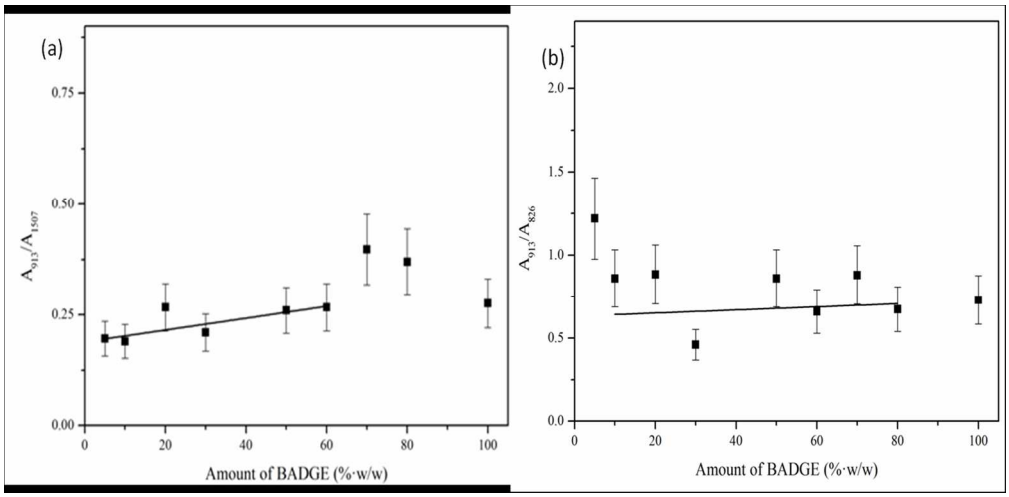

FTIR results for the epoxy index calculated using two peaks corresponding to oxirane ring of BADGE (a) epoxy index 1 (ep1) A913/A1507 against amount of BADGE, (b) epoxy index II (ep II) A913/A826 against amount of BADGE
248x120mm (150 x 150 DPI)

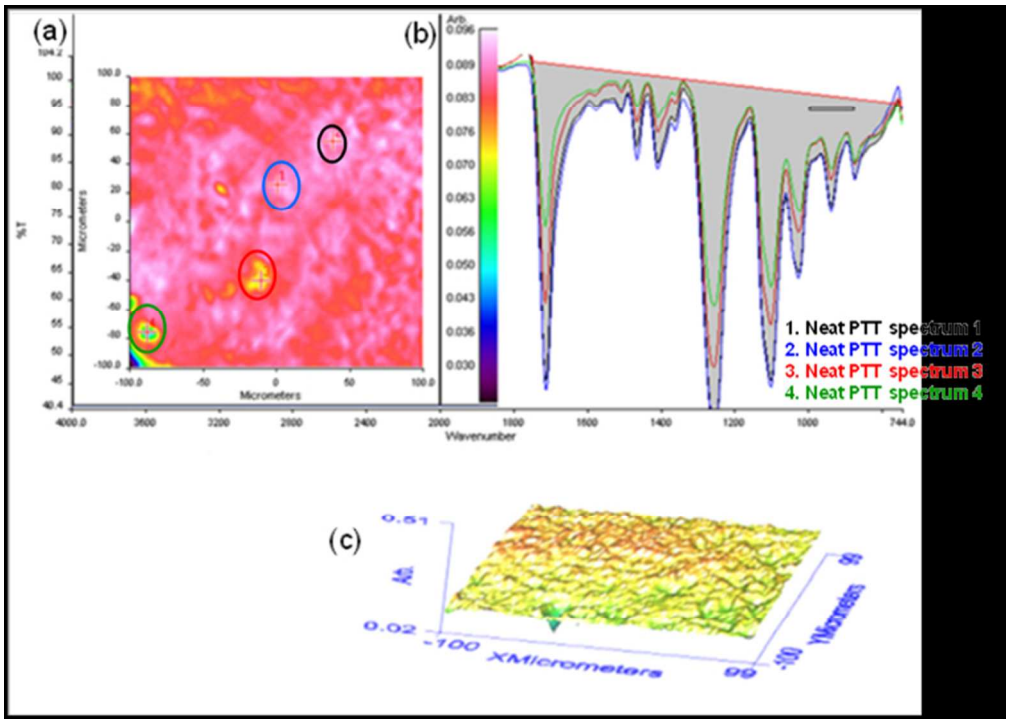

FTIR microscopy image for neat PTT (a) relative intensity of the distribution of the region between 1740-750 cm-1, (b) shows the relative intensity of the spectra, (c) shows the 3D projection image of the surface 220x157mm (87 x 87 DPI)

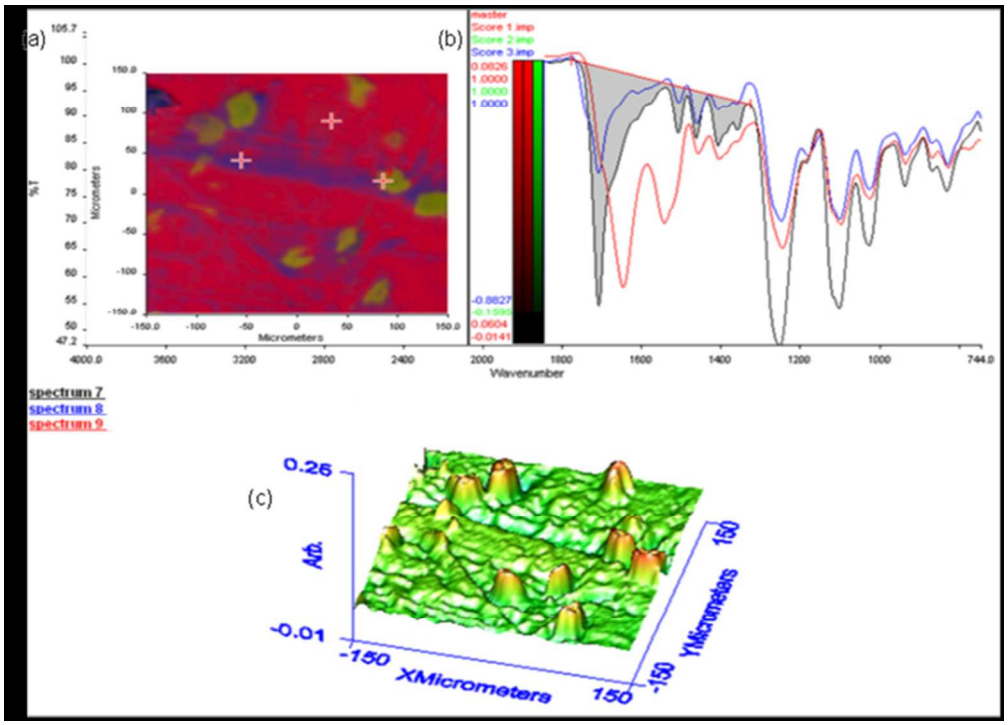

FTIR microscopy image for 70 %•w/w blend, (a) chemimap image of the region under investigation, (b) spectra from three different regions indicated in the chemimap, (c) 3D projection image of the region of interest
229x174mm (85 x 80 DPI)

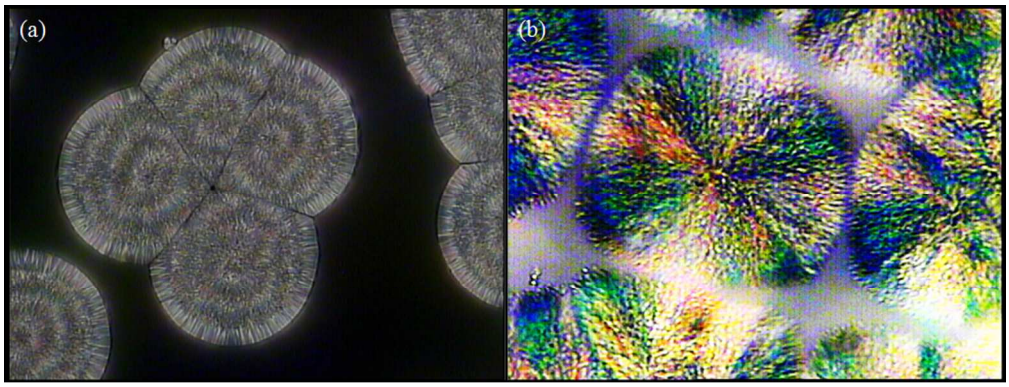

POM images of (a) neat PTT and (b) 50-50 blend at 198 °C after 1300 s at a scale bar of 25 μm
186x121mm (138 x 80 DPI)

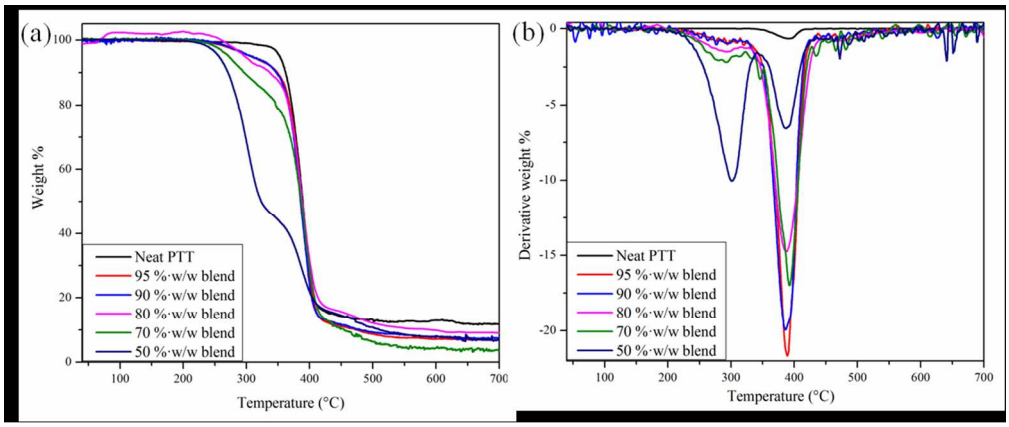

Plot of mass against temperature for PTT-BADGE blends, (a) shows a plot of the mass% as a function of temperature while (b) shows the derivative weight % as a function of temperature
325x135mm (110 x 110 DPI)

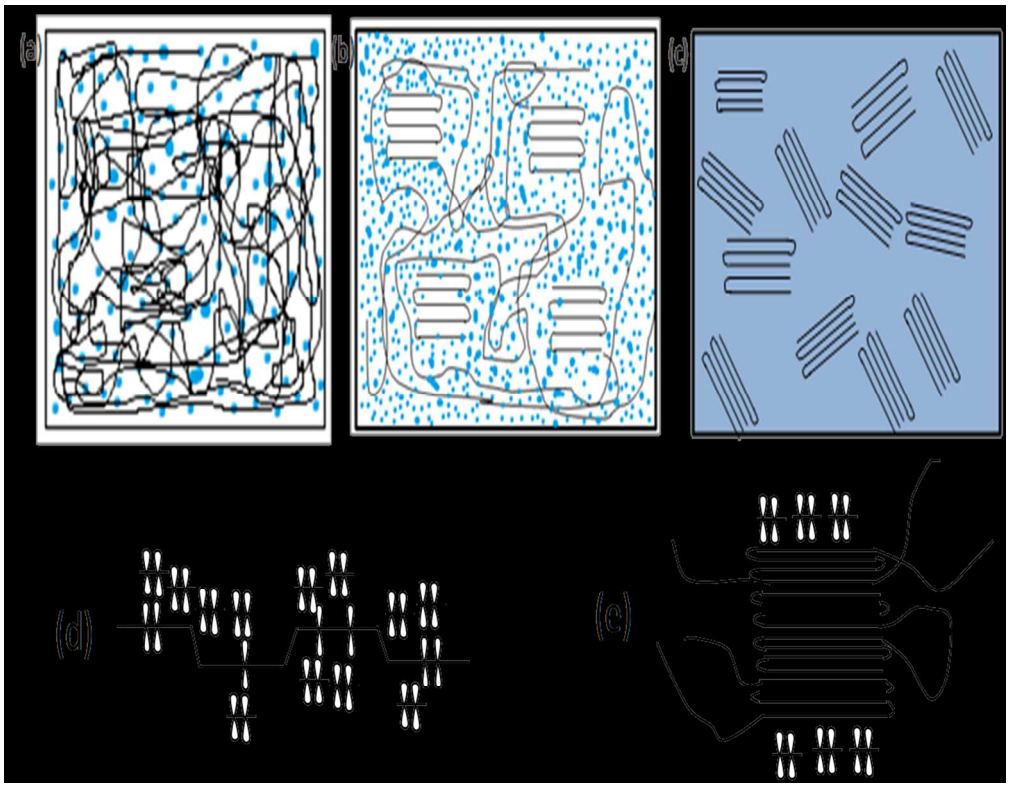

Schematic representation of the interaction between PTT and BADGE in the crystalline and amorphous regions of PTT. (a) represents the situation expected in the molten state, (b) shows the situation after the onset of crystallization, (c) represents the situation close to the endset of crystallization, (d) shows the reason expected for the interaction between PTT and amorphous BADGE monomers, (e) shows the reason for the immiscibility of the crystalline fraction of PTT with BADGE
216x167mm (150 x 150 DPI)